Hopper Growth of Salt Crystals

Julie Desarnaud[†,§,#]*, Hannelore Derluyn*[‡,#]*, Jan Carmeliet*[+,£] *, Daniel Bonn*[†]*, and Noushine Shahidzadeh*[*,†]

[†]Van der Waals-Zeeman Institute, Institute of Physics, University of Amsterdam, Science Park 904, 1098 XH Amsterdam, The Netherlands

[‡]CNRS/TOTAL/Univ Pau & Pays Adour/ E2S UPPA, Laboratoire des Fluides Complexes et leurs Réservoirs-IPRA, UMR5150, 64000 Pau, France

[+]Chair of Building Physics, ETH Zurich, Stefano-Franscini-Platz 5, 8093 Zürich Hönggerberg, Switzerland

[£]Laboratory for Building Science and Technology, EMPA, Swiss Federal Laboratories for Materials Science and Technology, Überlandstrasse 129, 8600 Dübendorf, Switzerland

SUPPORTING INFORMATION

The Supersaturation definition

We remark that to calculate K, we determine the best linear fit between the growth rate $G=dL/dt$ and the relative supersaturation S_m-1 (Eq. (1) where the supersaturation S_m represents the molality ratio m/m_0 (with m the molal concentration (mol.kg^{-1})). Thermodynamically, however, supersaturation is defined as an activity ratio[30,31,32], and the molality ratio is only an approximation. For electrolyte solutions, the mean ionic activity, $a_{\pm}$, is usually employed, defining the supersaturation as $S_a = a_{\pm}/a_{\pm,0}$. At high electrolyte concentrations, the supersaturation equals $S_a = \gamma_{\pm} m / \gamma_{\pm,0} m_0$, with m and $\gamma_{\pm}$, the molalities and mean activity

coefficients of the positive and negative ionic species, respectively. For dilute solutions of a 1-1 electrolyte, such as NaCl, the mean ionic activity is well approximated by the solution concentration and the supersaturation S_a is simply defined as the concentration ratio $S_m = {}^{m}/_{m_0}$. For a supersaturation range S_m between 1 and 2 at room temperature, i.e. the supersaturation range of our experiments, a linear relationship can be found between the relative supersaturations S_a-1 and S_m-1; i.e., $S_a - 1 \approx 2.43(S_m - 1)$ (with R^2=0.99), using the thermodynamic database from Steiger et al[33]. Using S_m or S_a to calculate K will thus only scale the growth coefficient with a constant value on a first-order approximation, and will have no influence on the activation energy estimated from the Arrhenius plot. Therefore, we opted in this paper to express all growth rates with respect to the relative supersaturation defined by the molality ratio S_m as this is the value that is directly obtained from experimental measurements without the need for a thermodynamic database.

Analysis of the literature data on overall growth rate coefficient K

Growth rate measurements of sodium chloride are scarce in the literature, and the data found are measured at low supersaturations for cubic habit crystals, employing different experimental techniques. Kubota et al.[22] used a flow cell to visualize the growth of single crystals under the microscope at 35°C. Supersaturation was created by changing the concentration of the NaCl solution. Rumford and Bain[18] report growth rates at 26, 38, 45, 52, 62 and 73°C, and Scrutton and Grootscholten[20] at 25, 40, 50, 60 and 75°C, derived from fluidized bed experiments where the bed was kept at a given temperatures and the incoming fluid was supersaturated with respect to this temperature by heating the solution bath to the required temperature to achieve the desired degree of supersaturation. Al-Jibbouri and Ulrich[23] and Ulrich et al.[26] used a fluidized bed as well, but they started from a saturated solution at 30°C and induced growth by cooling the bed. Ulrich et al.[26] also measured the growth rate of single NaCl crystals in a microscopic

cell. The crystals were immersed in a stagnant saturated solution of NaCl at 30°C, and growth was induced by cooling of the cell.

Depending on the consulted literature source, the growth rate is expressed as a mass deposition rate R_G (kg/m²s)[18,20,23] or as an overall linear growth rate G (m/s)[22,26]. The change of the length of the face of the cubic crystal L with time can be related to the change of the crystal mass with time by applying the shape factors method[34] and the relationship between the two growth rate quantities reads[32]:

$$R_G = \frac{1}{A}\frac{dM}{dt} = \frac{3\alpha}{\beta}\rho_c G = \frac{3\alpha}{\beta}\rho_c \frac{dL}{dt} \quad \text{(S1)}$$

where M is the crystal mass, A the crystal surface area and ρ_c the crystal density. For NaCl, ρ_c amounts 2165 kg/m^3. α and β are the volume and surface shape factors, respectively, with the volume of the crystal expressed as αL^3 and the surface of the crystal as βL^2. For cubic crystals, $6\alpha/\beta = 1$. The initial crystal shape and size are reported in some publications, as summarized in Table S1. When the crystal shape is not specified, a cubical crystal shape is assumed for the further calculations. The definition of the supersaturation differs as well. Some literature sources express supersaturation as concentration differences[18,20,23,26], whereas others speak of relative supersaturation[22]. The concentration difference $\Delta c = c - c_0$, with c_0 the equilibrium concentration, is expressed in mass or mole per volume unit or per mass unit. The relative supersaturation then equals $\Delta c/c_0$.

Table S1. Overview of the experimental settings and units reported in the literature

Source	T-range [°C]	Data	Crystal size & shape factors	Supersaturation	Method
1: Fig. 3 & 4	26, 38, 45, 52, 62, 73	R_G vs Δc	1.1 mm, cubical	Δc [kg/m³]	Fluidized bed; subcooling**
2: Fig. 4a	25, 40, 50, 60, 75	R_G vs Δc	780 µm; α=1, β=6 (p. 245)	Δc [kg/m³]	Fluidized bed; subcooling**
3: Table 1	30 → 25	R_G vs Δc	315-250 µm	Δc [kg/m³]	Fluidized bed; subcooling*
4: Fig. 1 & 2	30 → 25	G vs Δc	400-500 µm	Δc [g/100g H_2O]	Fluidized bed; subcooling*
4: Fig. 3	30 → 28.4	L vs time		Δc [g/100g H_2O]	Singe crystals in microscope cell; subcooling*

5: Fig. 2	35	G vs $\Delta c/c_0$		$\Delta c/c_0$ (c in [mol/dm³])	Singe crystals in microscope flow cell; subcooling**
Source	**Measurement time**	**Flow rate**	**Min (S_m-1)**	**Max (S_m-1)**	
1: Fig. 3 & 4	after 15 min.	3 cm s^{-1}	0.00195	0.01110	
2: Fig. 4a	after 4 to 20 min.	15 l h^{-1}	0.00075	0.01264	
3: Table 1	after 15 min.	not specified	0.00071	0.00338	
4: Fig. 1 & 2	after 10 min.	not specified	0.00062	0.00354	
4: Fig. 3	6 points between 1 and 20 min. for 4 crystals	stagnant	0.00111	0.00111	
5: Fig. 2	after 30 min.	13.3 cm s^{-1}	0.00554	0.01262	

*: by cooling of the cell/bed

**: by injecting solution saturated at higher temperature

1: Rumford & Bain 1960[18]; 2: Scrutton & Grootscholten 1980[20]; 3: Al-Jibbouri & Ulrich 2002[23]; 4: Ulrich et al. 1993[26]; 5: Kubota et al. 2000[22].

To compare the literature data with the data obtained in this work, all R_G growth rate values reported in the literature were recalculated to overall linear growth rates G applying Eq. (S1). All concentrations were recalculated to molal concentrations. For literature sources only reporting concentrations per unit of volume[20,22], the subcooling was inferred from the solubility and density expressions given in the article (p. 239) in the case of Scrutton and Grootscholten[20], and from the solubility and density predicted by the thermodynamic database of Steiger *et al.*[33,35] in the case of Kubota *et al*[22]. The molal concentrations then correspond to the solubility values (in molal) at the respective temperatures as obtained from Steiger's database[33]. For sources reporting the subcooling values[18,23], the molal solubilities are directly calculated using the same database[33]. Mass fractions[26] (in mass/mass water) were transformed into molalities by dividing by the molar mass of NaCl of 58.4428 g/mol. The corresponding minimal and maximal relative supersaturations as defined in this paper, S_m-1, are given in Table S1 for each dataset. The values range from 0.0006 up to 0.013.

The classical Burton-Cabreba-Frank (BCF) theory of crystal growth

The BCF theory describes the growth when the rate-limiting step for the growth of a crystal is the incorporation of molecules in the crystal lattice. To compare our results with BCF, in Fig. SI1, we plot the cubic growth rates measured in the first seconds (dL_F/dt for t<20 sec) as a

function of the relative supersaturation achieved at the onset of precipitation, as shown in Fig. 4a.

The BCF theory gives[36]

$$\frac{\mathrm{dL}}{\mathrm{dt}} = \frac{\mathrm{C}}{\sigma_c}\sigma_i^2 \tanh\left(\frac{\sigma_c}{\sigma_i}\right) \tag{S2}$$

where C and $\sigma_c \approx 0.025$[37] are parameters of the model, and $\sigma_i \approx \mathrm{S_m} - 1$ represents the relative supersaturation next to the surface of the growing crystal. Since we are concerned with the initial growth, σ_i can be considered close to the supersaturation for which the crystal is first observed. It is usual to represent this in reduced coordinates, $R_r = \sigma_r \tanh\left(\frac{1}{\sigma_r}\right)$, with the reduced growth rate $R_r = \frac{\mathrm{dL}}{\mathrm{dt}}/\mathrm{C}\sigma_i$ and the reduce supersaturation $\sigma_r = \sigma_i/\sigma_c$. Reducing the experimental data in this same way allows for a comparison and shows that the BCF theory describes the data in a satisfactory manner (Fig. SI1). The linear relationship found in our experiments in Fig. 4a) i.e. g=1, also follows from the BCF equation; when the argument of the hyperbolic tangent is small, it can be expanded as $\tanh\left(\frac{\sigma_c}{\sigma_i}\right) \sim \left(\frac{\sigma_c}{\sigma_i}\right)$ and the linear growth rate is recovered.

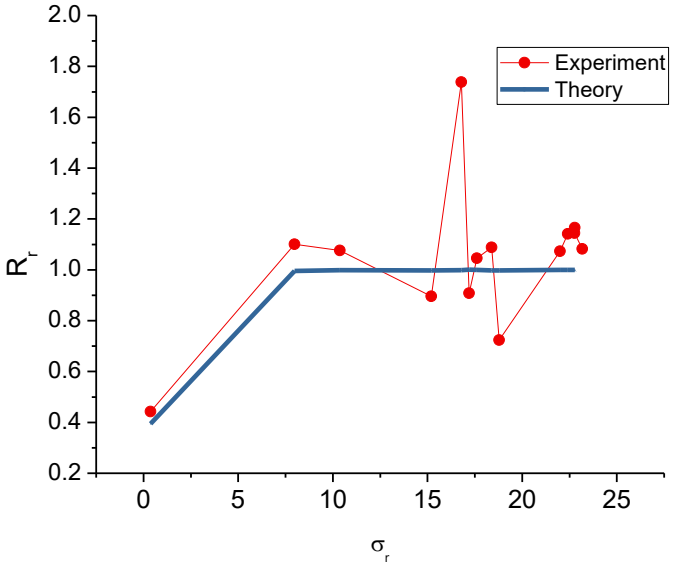

Figure SI1-. Comparison in reduced units between BCF theory and experimental data. The reduced units are explained in the text; the red points are the experimental data, and the blue ones are the BCF model.

AUTHOR INFORMATION

Corresponding Author

* E-mail: n.shahidzadeh@uva.nl

Present address

[§]*J.Desarnaud Getty Conservation Institute, 1200 Getty Center Drive, Suite 700, Los Angeles, California*
90049, USA

REFERENCES

(1) Desarnaud, J.; Bonn, D.; Shahidzadeh, N. Measurement of the Pressure Induced by Salt Crystallization in Confinement. *Sci. Rep.* **2016**, *6*, 30856.

(2) Desarnaud, J.; Derluyn, H.; Molari, L.; de Miranda, S.; Cnudde, V.; Shahidzadeh, N. Drying of Salt Contaminated Porous Media: Effect of Primary and Secondary Nucleation. *J. Appl. Phys.* **2015**, *118* (11), 114901.

(3) Shahidzadeh-Bonn, N.; Desarnaud, J.; Bertrand, F.; Chateau, X.; Bonn, D. Damage in Porous Media Due to Salt Crystallization. *Phys. Rev. E* **2010**, *81* (6), 1–6.

(4) Braga, D.; Grepioni, F.; Maini, L.; Polito, M. Crystal Polymorphism and Multiple Crystal Forms. In *Molecular Networks. Structure and Bonding.*; Hosseini, M., Ed.; Springer, Berlin, Heidelberg, 2009; Vol. 132, pp 87–95.

(5) Rasenack, N.; Müller, B. W. Crystal Habit and Tableting Behavior. *Int. J. Pharm.* **2002**, *244*, 45–57.

(6) Quilaqueo, M.; Duizer, L.; Aguilera, J. M. The Morphology of Salt Crystals Affects the Perception of Saltiness. *Food Res. Int.* **2015**, *76*, 675–681.

(7) Zhang, J.; Zhang, S.; Wang, Z.; Zhang, Z.; Wang, S.; Wang, S. Hopper-like Single Crystals of Sodium Chloride Grown at the Interface of Metastable Water Droplets. *Angew. Chemie - Int. Ed.* **2011**, *50* (27), 6044–6047.

(8) Fontana, P.; Pettit, D.; Cristoforetti, S. Sodium Chloride Crystallization from Thin Liquid Sheets, Thick Layers, and Sessile Drops in Microgravity. *J. Cryst. Growth* **2015**, *428*, 80–85.

(9) Fontana, P. *Die Vielfalt Der Salzkristalle*; R + A Print, 2013.

(10) Desarnaud, J.; Derluyn, H.; Carmeliet, J.; Bonn, D.; Shahidzadeh, N. Metastability Limit for the Nucleation of NaCl Crystals in Confinement. *J. Phys. Chem. Lett.* **2014**, *5*, 890–895.

(11) Shahidzadeh, N.; Schut, M. F. L.; Desarnaud, J.; Prat, M.; Bonn, D. Salt Stains from Evaporating Droplets. *Sci. Rep.* **2015**, *5*, 10335.

(12) Qazi, M. J.; Liefferink, R. W.; Schlegel, S. J.; Backus, E. H. G.; Bonn, D.; Shahidzadeh, N. Influence of Surfactants on Sodium Chloride Crystallization in Confinement. *Langmuir* **2017**, *33* (17), 4260–4268.

(13) Naillon, A.; Duru, P.; Marcoux, M.; Prat, M. Evaporation with Sodium Chloride Crystallization in a Capillary Tube. *J. Cryst. Growth* **2015**, *422*, 52–61.

(14) Zahn, D. Atomistic Mechanism of NaCl Nucleation from an Aqueous Solution. *Phys. Rev. Lett.* **2004**, *92* (4), 1–4.

(15) Mucha, M.; Jungwirth, P. Salt Crystallization from an Evaporating Aqueous Solution by Molecular Dynamics Simulations. *J. Chem. Phys. B* **2003**, *107* (33), 8271–8274.

(16) Chakraborty, D.; Patey, G. N. How Crystals Nucleate and Grow in Aqueous NaCl Solution. *J. Phys. Chem. Lett.* **2013**, *4*, 573–578.

(17) Chakraborty, D.; Patey, G. N. Evidence That Crystal Nucleation in Aqueous NaCl Solution Occurs by the Two-Step Mechanism. *Chem. Phys. Lett.* **2013**, *587*, 25–29.

(18) Rumford, F.; Bain, J. The Controlled Crystallization of Sodium Chloride. *Trans. Inst. Chem. Eng.* **1960**, *38*, 10–20.

(19) Sunagawa, I.; Tsukamoto, K. Growth Spirals on NaCl and KCl Crystals Grown from Solution. *J. Cryst. Growth* **1972**, *15*, 73–78.

(20) Scrutton, A.; Grootscholten, P. A. M. A Study on the Dissolution and Growth of Sodium Chloride Crystals. *Trans. Inst. Chem. Eng.* **1981**, *59*, 238–246.

(21) Ulrich, J.; Mohameed, H.; Zhang, S.-B.; Yuan, J.-J. Effect of Additives on the Crystal Growth Rates: Case Study NaCl. *Bulltetin Soc. Sea Water Sci. Japan* **1997**, *51* (2), 73–77.

(22) Kubota, N.; Otosaka, H.; Doki, N.; Yokota, M.; Sato, A. Effect of Lead(II) Impurity on the Growth of Sodium Chloride Crystals. *J. Cryst. Growth* **2000**, *220*, 135–139.

(23) Al-Jibbouri, S.; Ulrich, J. The Growth and Dissolution of Sodium Chloride in a Fluidized Bed Crystallizer. *J. Cryst. Growth* **2002**, *234*, 237–246.

(24) Linnikov, O. D. Spontaneous Crystallization of Sodium Chloride from Aqueous-Ethanol Solutions. Part 1: Kinetics and Mechanism of the Crystallization Process. *Cryst. Res. Technol.* **2006**, *41* (1), 10–17.

(25) Zhao, J.; Miao, H.; Duan, L.; Kang, Q.; He, L. The Mass Transfer Process and the Growth Rate of NaCl Crystal Growth by Evaporation Based on Temporal Phase Evaluation. *Opt. Lasers Eng.* **2012**, *50* (4), 540–546.

(26) Ulrich, J.; Kruse, M.; Stepanski, M. On The Growth Behaviour of NaCl Crystals With and Without Additives. In *Seventh Symposium on Salt*; Elsevier Science Publishers B.V., Amsterdam, 1993; Vol. II, pp 209–212.

(27) Okada, I.; Namiki, Y.; Uchida, H.; Aizawa, M.; Itatani, K. MD Simulation of Crystal

Growth of NaCl from Its Supersaturated Aqueous Solution. *J. Mol. Liq.* **2005**, *118*, 131–139.

(28) Grossier, R.; Veesler, S. Reaching One Single and Stable Critical Cluster through Finite-Sized Systems. *Cryst. Growth Des.* **2009**, *9* (4), 1917–1922.

(29) Naillon, A.; Joseph, P.; Prat, M. Sodium Chloride Precipitation Reaction Coefficient from Crystallization Experiment in a Microfluidic Device. *J. Cryst. Growth* **2017**, *463*, 201–210.

(30) Nielsen, A. E.; Toft, J. M. Electrolyte Crystal Growth Kinetics. *J. Cryst. Growth* **1984**, *67*, 278–288.

(31) Nielsen, A. E. Electrolyte Crystal Growth Mechanisms. *J. Cryst. Growth* **1984**, *67*, 289–310.

(32) Mullin, J. W. *Crystallization*, 4th ed.; Butterworth-Heinemann: Oxford, 2001.

(33) Steiger, M.; Kiekbusch, J.; Nicolai, A. An Improved Model Incorporating Pitzer's Equations for Calculation of Thermodynamic Properties of Pore Solutions Implemented into an Efficient Program Code. *Constr. Build. Mater.* **2008**, *22* (8), 1841–1850.

(34) Nývlt, J.; Matuchová, M. Determination of Linear Growth Rates of Crystals (II). The Shape Factors Method. *Krist. und Tech.* **1976**, *11* (3), 245–253.

(35) Steiger, M. Chapter 6: Total Volumes of Crystalline Solids and Salt Solutions. In *An expert chemical model for determining the environmental conditions needed to prevent salt damage in porous materials*; Price, C., Ed.; 2000; Vol. 0135, pp 53–63.

(36) Ghez, R. *A Primer of Diffusion Problems*; John Wiley & Sons, Inc., 2005.

(37) Tai, C. Y.; Cheng, C.; Huang, Y. Interpretation of Crystal Growth Rate Data Using a Modified Two-Step Model. *J. Cryst. Growth* **1992**, *123*, 236–246.